KSTLE International Journal, Vol. 4, No. 1, June 2003, pp. 1-7

A Study on the Rotordynamic Stability of Turbo Pump Unit

Hyun-Duck Kwak, Yong-Bok Lee†, Chang-Ho Kim, Tae-Woong Ha* and Woo-Chul Yoo**
Tribology Research Center, Korea Institute of Science and Technology
**Department of Mechanical Engineering, Kyungwon Univ.*
***Hyundai Mobis Co.*

Abstract: A turbo pump unit provides high pressure oxygen and fuel in a space shuttle main engine (SSME). This paper focused on rotordynamics, investigating its characteristics based on a numerical simulation of turbo pump finite element model. Speeds up to 50,000 rpm are considered, as well as the special problems related to elastic-ring, seal hydrodynamic force, shroud force and clearance-excitation force. The rotordynamic prediction shows that the elastic-ring which is inserted between the casing and the outer race of ball bearing allows for an acceptable separate margin of first critical speed. Additionally, the results show that the floating ring seal, which have a peculiar ring, adds substantial stiffness and damping to the system as well as exhibits superior performance in terms of rotordynamic stability of system compared to the plain seal.

Keywords: Turbo pump, elastic-ring, plain seal, floating ring seal, stability

Introduction

A turbo pump unit concerned herein provides cryogenic liquid oxygen and fuel to combustors in liquid rocket engines. For successful development of turbo pump units, concurrent design including thermodynamic, hydraulic, dynamic and material considerations is crucial. Generally, in the process of design, one must carefully consider the system reliability because the turbo pump unit usually operates in severe circumstances. Especially, from the standpoint of rotordynamics, a rotordynamic stability of the system should be guaranteed.

Given this background, many studies confirming or improving the stability of turbo pump unit have been widely conducted. Regarding bearing elements, several researches reported characteristics of hydrostatic or liquid foil bearings for the replacement of ball bearings. Braun *et al.* [1] performed an integrated analysis of the behavior of hydrostatic cryogenic bearing used by turbo pump of the space shuttle main engine (SSME), and clarified the static characteristics. Similarly, Yoshikawa *et al.* [2] characterized the dynamic behavior of hydrostatic cryogenic bearing. Relating more to rotordynamics, Fayolle and Childs [3] experimentally investigated a roughened-land hybrid bearing focused on reducing a destabilizing forces. Saville *et al.* [4] performed an experimental study on liquid foil bearing and represented that its rotordynamic stability to be superior. In addition, several studies were conducted relating to improving of rotordynamic performance of seals used in turbo pump units. Childs and Kim [5] proposed the optimum configurations and dimensions of round-hole-pattern damper seals for maximum net damping. In addition, they found that helically-grooved annular seals have pronounced rotordynamic stability advantages. [6] However, rotordynamic stability of the turbo pump unit depends on dynamics of whole system including critical speeds, onset speed of instability (OSI) and time-transient response as well as the rotordynamic elements such as bearings and seals. In this respect, Childs [7] demonstrated that the rotordynamic instability problem of SSME fuel turbo pump including bearings, seals, internal rotor damping and casing dynamics. As a result, he proposed that the asymmetric design is more stable with synchronous response characteristics than the stiffly supported design.

This paper is concerned with the development and analysis of rotordynamic models for the high pressure oxygen turbo pump (HPOTP) and the high pressure fuel turbo pump (HPFTP). Elements of rotordynamic model which are discussed in detail include stiffness of ball bearings and elastic-ring, hydrodynamic forces due to seals, shroud forces of impellers and clearance-excitation forces due to turbine. Especially, concentrated on seal elements, the influence of seal type on system dynamics is investigated for improving a rotordynamic stability of turbo pump unit.

Schematics of Turbo Pump Unit

The rotating elements assembly of turbo pump unit is illustrated in Fig. 1. In terms of rotordynamics, the turbo pump considered herein is mainly composed of three sections - liquid oxygen (LO_2) pump, liquid fuel (LCH_4) pump and driven turbine. In the liquid oxygen pump, there are booster inducer, inducer and impeller as hydraulic components. The booster inducer and inducer diameters in liquid oxygen pump are about 40 mm and 50 mm, respectively. Pump discharge pressure is 14.75 MPa with a mass flow rate of 24.34 kg/sec at full power level speed. Similar to liquid oxygen pump, the

†Corresponding author; Tel: 82-2-958-5663, Fax: 82-2-958-5659
E-mail: lyb@kist.re.kr

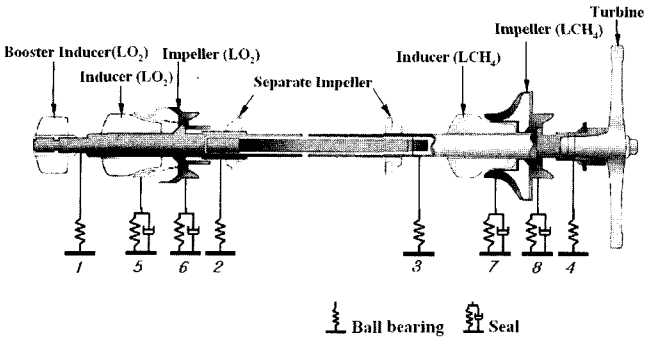

Fig. 1. Rotating elements assembly of high pressure oxygen turbo pump (HPOTP) and high pressure fuel turbo pump (HPFTP).

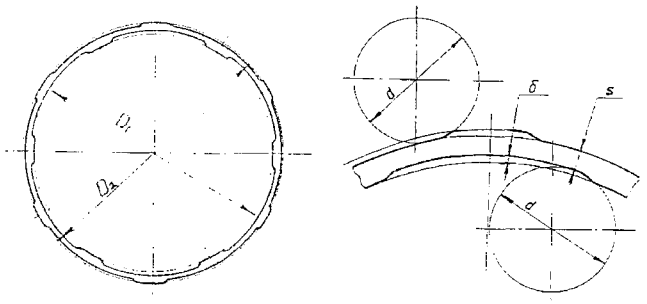

Fig. 2. Configuration of elastic-ring.

liquid fuel pump section consists of an inducer and impeller but does not have a booster inducer. Inducer diameter of liquid fuel pump is about 58 mm. Pump discharge pressure of liquid fuel pump is 15 MPa with a mass flow rate of 9.05 kg/sec. The liquid oxygen and fuel pumps are connected by a spline coupling. The turbine section develops about 1057 kW at a full power level speed of 50,000 rpm. Two separate impellers on the ends of spline coupling prevent liquid oxygen and fuel from mixing. The total system of rotating elements is about 470 mm long and weighs about 4.0 kg. To provide stiffness for the system, four ball bearings are used. The smallest one is located between the booster inducer and inducer of liquid oxygen pump (No. 1) and the largest one is situated between the liquid fuel pump and turbine (No. 4). Additionally, two ball bearings of same size (No. 2 and 3) are located on the ends of spline coupling. Finally, a pair of seals minimizes leakage flow in oxygen and fuel pump in addition to providing additional stiffness and damping to the turbo pump unit.

Rotordynamic Model of Turbo Pump Unit

Stiffness of ball bearing with elastic-ring

As described previously, there are four ball bearings in turbo pump unit. The No. 1 and 2 bearings are cooled by liquid oxygen, while the other bearings of No. 3 and 4 are cooled by liquid fuel. In terms of rotordynamics, stiffness and damping coefficients of the ball bearings are considerable. In this paper, the direct stiffness of the ball bearing is calculated based on radial load versus radial displacement curves [8]. By extracting slope from these curves, the direct stiffness of the ball bearings is formulated. The results are shown Table 1. The damping of ball bearing is neglected.

Figure 2 represents the elastic-ring, which is inserted between the outer race of ball bearing No. 4 and the casing of the turbo pump unit. The elastic-ring is made up of a simple steel ring with an arbitrary number of grooves on its inner and outer surfaces. By controlling the geometric parameters of grooves including depth, width and radius of curvature, the stiffness of the elastic-ring is adjustable. The stiffness of elastic-ring is calculated from an empirical equation, which can be expressed in terms of compliance as follows (8).

$$\alpha = \frac{D_{cp} - 0.3b_1 nb}{0.129bEn^4 s^3}\left(1 - \left(1 - \frac{s^3}{s_b^3}\right)\right)(1.45A - 0.9A^2 + 0.2A^3) \tag{1}$$

From equation (1), the stiffness of elastic-ring can be calculated as a value of 8.3312×10^6 N/m. Because the elastic-ring is inserted on the outer race of ball bearing No. 4, it can be concluded that two springs are serially connected. Thus, the resultant stiffness of bearing No. 4 can be readily found from equation (2).

$$\frac{1}{K_{total}} = \frac{1}{K_{ring}} + \frac{1}{K_{brg}} \tag{2}$$

Rotordynamic coefficients of seals

The major function of seals in a pump system is to isolate a working medium. Generally, high speed rotating machinery uses non-contact shaft seals for isolation because a surface friction force significantly reduces system efficiency. However, non-contact seals lead a leakage flow of working medium as well as dynamic forces due to their radial clearance. Experience has demonstrated that pump seals have a great influence on pump rotordynamic characteristics [9,10,11]. Thus, seal design could be an important factor in rotordynamic stability. Therefore, in this paper, two types of seals, the plain

Table 1. Ball bearings properties

Number	1	2 and 3	4
Location	LO_2 pump	LO_2 & LCH_4 pump	LCH_4 pump
Dimension (mm) (d × D × b)	10 × 26 × 8	20 × 47 × 14	25 × 52 × 15
Radial Stiffness (N/m)	2.312×10^7	6.679×10^7	8.222×10^7
Cooling Medium	LO_2	LO_2, LCH_4	LCH_4

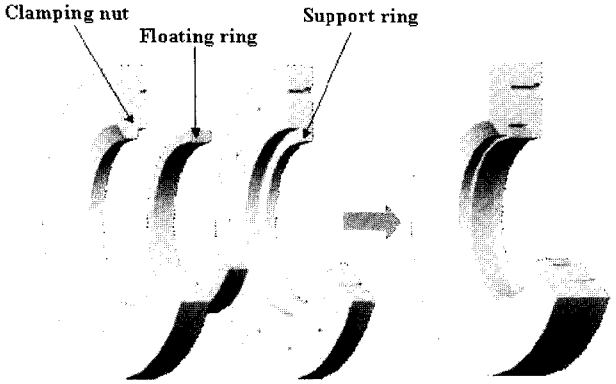

Fig. 3. Floating ring seal.

seal and the floating ring seal, are considered for the use in turbo pump unit.

The estimation of rotordynamic coefficients of the plain seal is based on the Kim's work [12]. He developed the solution procedure of seals with various surface configurations using empirical coefficients. In present analysis, the rotordynamic coefficients were extracted by using the empirical coefficients of the plain seal that suggested in his work. Figure 3 represents the structural arrangement of the floating ring seal. The floating ring is inserted between the rotor and the pump housing and its axial motion is restrained by a clamping nut. The floating ring is in contact with the rotor surface at the maximum eccentricity position when the pump is not operating. When the pump begins to operate, the pressure induced by the back-flow liquid (from the outlet of the impeller to the front shroud) attaches the floating ring to the supporting ring surface. Simultaneously, the hydrodynamic force in a radial direction is generated by the eccentricity. This force moves the floating ring to the geometric center of the rotor. After the hydrodynamic force and the friction force achieve equilibrium, the floating ring is locked-up at that eccentricity. At that time, the floating ring seal begins to act like an eccentric annular plain seal. Thus, it is possible to maintain a minimum radial clearance without any rubbing. A numerical analysis of rotordynamic coefficients of the floating ring seal concerned herein was initiated by Ha *et al.* [13] Based on the 'bulk flow model', they developed a solution using Nelson and Nguyen's Fast Fourier Transform Method [14] and presented their results including lock-up position, attitude angle, leakage flow rate, and rotordynamic coefficients. In this paper, the rotordynamic coefficients of floating ring seals in turbo pump unit are cited from their results.

Rotordynamic coefficients of impeller shrouds

As noted previously, there are two pumps of a liquid oxygen pump and a liquid fuel pump in turbo pump unit concerning herein. The liquid oxygen pump impeller is shrouded with its front and rear impeller shrouds symmetrical. Leakage along the front and rear impeller shroud, from the impeller discharge to the inlet, is restricted by the front and the rear seals respectively. The lateral hydrodynamic forces are developed along the front and the rear impeller shrouds. The impeller of the liquid fuel pump is also shrouded. However, the lateral hydrodynamic forces are only developed along the front impeller shroud due to its geometrical design. The rotordynamic analysis of the impeller shroud was developed by Ha and Lee [15] based on Hirs' bulk-flow model approach and Blasius' surface friction factor model for a concentric rotor. The rotordynamic coefficient results for the shrouds, by using the code of Ha and Lee [15], are listed in Table 2. At the full power level speed, the rotordynamic coefficients of shrouds are very small compared to those of plain or floating ring seals due to their relatively short length and large shroud clearance, which yields less than 1%. Thus, the rotordynamic coefficients were neglected in this analysis.

Clearance-excitation forces

Because a turbine carries the large amount of concentrated power, this element has been suspected of making a large contribution to destabilizing forces. Thomas [16] initially suggested that asymmetric clearances caused by eccentric operation of a turbine could create destabilizing forces. Similarly, Alford [17] identified the same mechanism while analyzing stability of aircraft gas turbines. These destabilizing forces are called clearance-excitation forces or Alford forces. The clearance-excitation force provides a pure cross-coupled stiffness that destabilizes a system without direct stiffness or damping. In this paper, the Alford model is used for the calculation of the turbine rotordynamic coefficient, which is defined as follows.

$$k_t = \frac{T\beta}{D_m L_t} \tag{3}$$

In calculating cross-coupled stiffness using equation (3), the turbine torque is extracted from experimental data and the is assumed to be 1.0. As a result, the turbine cross-coupled stiffness is estimated to be about 7.0×10^4 N/m at full power level speed of turbo pump unit.

Table 2. Rotordynamic coefficients of impeller shrouds at the full power level speed of turbo pump unit

	Front Impeller Shroud of LO_2 Pump	Rear Impeller Shroud of LO_2 Pump	Front Impeller Shroud of LCH_4 Pump
K (N/m)	-227.8	-273.0	-58544
k (N/m)	7256.4	9689.6	56848
C (N-s/m)	4.8	6.3	18.3
c (N-s/m)	0.5	0.7	27.3

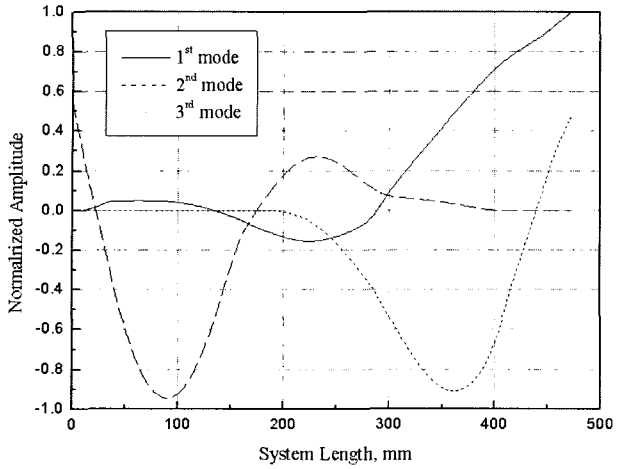

Fig. 4. Natural modes of turbo pump unit.

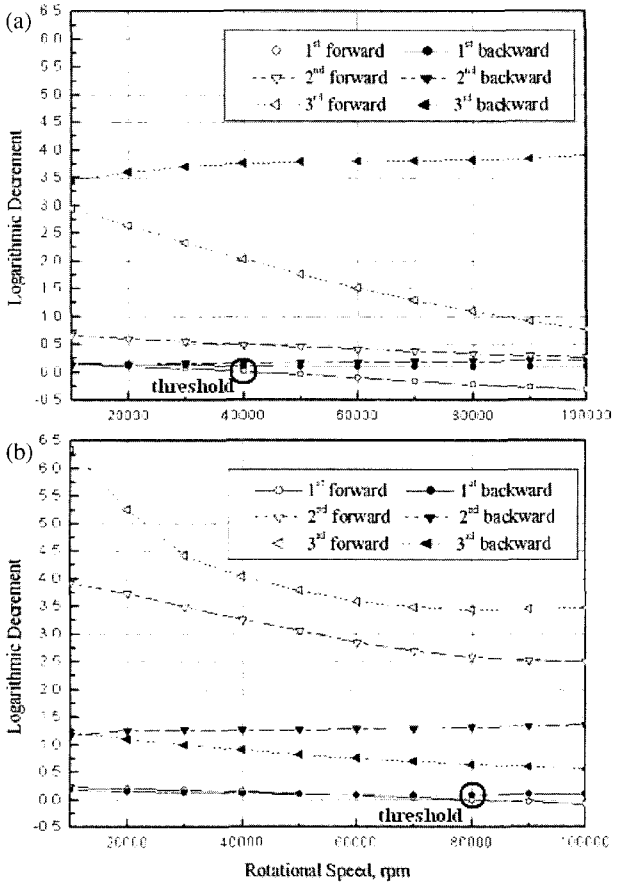

Fig. 5. Logarithmic decrement threshold prediction: (a) plain seal applied case (b) floating ring seal applied case.

Finite element model of turbo pump unit for rotordynamic analysis

The system has been discretisized into 20 nodes in an axial direction. Euler-Bernoulli beam elements have been used to connect the nodes, anisotropic springs and dampers to represents the bearings, seals and turbine. Each node is represented by four degrees of freedom and the spline coupling is modeled as a pin joint that only transfers a shear force except a moment across the node. All mass inertia elements including inducers, impellers and turbine are modeled as disk elements with a gyroscopic effect and those polar and transverse moments of inertia are calculated computationally based on the actual 3D models.

Rotordynamic Predictions of Two Cases of Turbo Pump Unit Configurations

Influence of elastic-ring on critical speeds

Table 3 represents the predicted critical speeds of turbo pump unit. Total four cases of system are considered. Initially, the first critical speeds of the turbo pump without elastic-ring are about 60,000 rpm. The first critical speeds of plain seals applied to the turbo pump and floating ring seals applied to the turbo pump are 59,830 and 60,822 rpm, respectively. Recalling that the full power level speed is 50,000 rpm, the separate margin of first critical speed is less than 20%, which leads to the possibility of excessive vibration during its operation. Figure 4 provides the natural mode of turbo pump at the first critical speed, which is a turbine-bending mode. Thus to obtain an acceptable separate margin, the turbine support stiffness should be increased or decreased. In this work, turbine support stiffness was decreased by inserting the elastic-ring between the outer race of turbine ball bearing and the casing. The elastic-ring, which has a relatively small stiffness compared to ball bearing, achieves a more separate margin. Table 3 shows that the first critical speeds of turbo pump with elastic-ring have been reduced to 21,289 and 22,380 rpm for both plain and floating ring seal cases. However, the second and third critical speeds have the appropriate separate margin, approximately 54% and 74% to avoid a resonance during operation.

Rotordynamic stability

From the standpoint of stability, the logarithmic decrements of system are of interest; specifically, a negative logarithmic decrement means that the system is linearly unstable. Figure 5

Table 3. Predicted critical speeds of turbo pump unit

Critical Speeds (rpm)	Without Elastic-ring		With Elastic-ring		Bending Location
	Plain	Floating Ring	Plain	Floating Ring	
1st	59830	60822	21289	22380	Turbine
2nd	83297	84026	84421	85042	LO_2 Pump
3rd	87304	91349	87589	90683	LCH_4 Pump

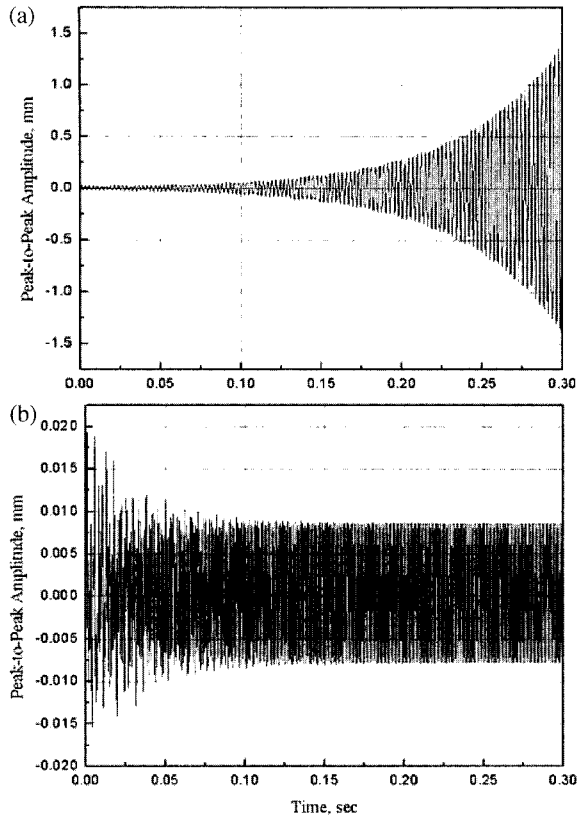

Fig. 6. Turbine peak-to-peak amplitude versus time at 50,000 rpm: (a) plain seal applied case (b) floating ring seal applied case.

shows the logarithmic decrement versus speed plot. Instability is predicted for the first forward critical speed associated with the turbine-bending mode of Table 3. The predicted onset speeds of instability (OSI) are around 40,000 rpm for plain seal and 80,000 rpm for floating ring seal case, respectively. This result signifies that the plain seal does not provide a stable operating at the full power level speed of turbo pump unit. To clarify this result, a time-transient response analysis at turbine was performed. Figure 6 illustrates comparable simulations for plain and floating ring seals. At the full power level speed, beyond the instability threshold of plain seal, the time-transient response of plain seal diverges rapidly. Thus, the turbo pump unit with plain seals is unstable at its full power level speed. However, the turbo pump unit with floating ring seals shows a stable response with 0.02 mm of peak-to-peak amplitude.

The number of frequency responses due to rotor whirling is illustrated by the Fourier spectra in Fig. 7. All waterfall plots are based on X components of whirling orbit. Synchronous response with running speed is evident in all of the spectra. As shown in Fig. 7 (a) and (b), a large synchronous response appears around 20,000 rpm due to the influence of first critical speed. However, this synchronous response peak does not appear at oxygen pump because the first critical speed is associated with the turbine-bending mode. Beyond the first critical speed, the responses of the turbine and fuel pump split into three frequency components, while the synchronous response dominates in the oxygen pump. The sub-synchronous responses are around 250 Hz and 400 Hz. The sub-synchronous response of 400 Hz at turbine, in particular, increases rapidly with speed.

At over 80,000 rpm, this sub-synchronous response diverges. Similarly, the sub-synchronous response of 400 Hz at fuel pump also diverges. This phenomenon is related to the

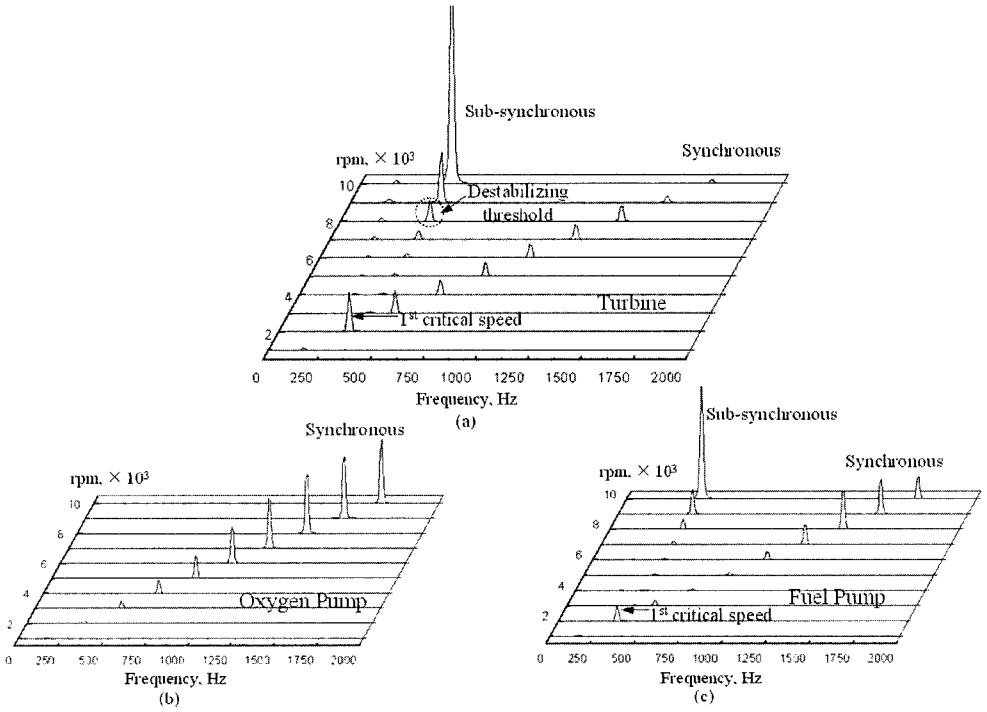

Fig. 7. Waterfall plot of Fourier spectra due to the whirling of rotor for the floating ring seal applied turbo pump unit: (a) turbine (b) oxygen pump (c) fuel pump.

instability predicted in Fig. 5. Remind that the instability threshold of floating ring seal case is 80,000 rpm, it is obvious that the sub-synchronous response of 400 Hz is caused by destabilizing forces of system. However, the sub-synchronous response of 250 Hz is relatively small compared to that of 400 Hz.

Conclusions

For the turbo pump unit in liquid rocket engine, the rotordynamic models were developed and analysed. Two case studies, plain seal applied turbo pump unit and floating ring seal applied turbo pump unit, were performed to compare rotordynamic characteristics and to evaluate appropriate design configuration. From the critical speeds analysis, it was found that there was a possibility of excessive vibration problem due to the first critical speed. By inserting the elastic-ring between the bearing and casing to reduce the support stiffness, this problem was remedied. The results of the synchronous response prediction indicated that the floating ring seal applied turbo pump unit was relatively superior to the plain seal applied turbo pump unit. In terms of stability, the plain seal applied turbo pump unit was shown to be unstable, while the floating ring seal applied turbo pump was marginally stable. The results of the present study support the conclusion that the floating ring seal applied turbo pump unit could successfully operate at its full power level speed, 50,000 rpm.

Acknowledgments

This study was sponsored by a grant from the Dual Use Technology Program and KSLV-I Program of the Ministry of Science and Technology, Republic of Korea.

References

1. Braun M. J., Wheeler R. L. and Hendricks R. C., "A Fully Coupled Variable Properties Thermohydraulic Model for a Cryogenic Hydrostatic Journal Bearing", ASME Journal of Tribology, Vol. 109, pp. 405-416, 1987.
2. Yoshikawa H., Ota T., Higashino K., and Nakai S., "Numerical Analysis on Dynamic Characteristics of Cryogenic Hydrostatic Journal Bearing", ASME Journal of Tribology, Vol. 121, pp. 879-885, 1999.
3. Fayolle P., and Childs D. W., "Rotordynamic Evaluation of a Roughened-Land Hybrid Bearing", ASME Journal of Tribology, Vol. 121, pp. 133-138, 1999.
4. Saville M., Gu A., and Capaldi R., "Liquid Hydrogen Turbopump Foil Bearing", AIAA/SAE/ASME/ASEE 27th Joint Propulsion Conference, AIAA-91-2108-CP, Sacramento, CA, 1991.
5. Childs D. W. and Kim C. H., "Test Results For Round-Hole-Pattern Damper Seals: Optimum Configurations and Dimensions for Maximum Net Damping", ASME Journal of Tribology, Vol. 108, pp. 605-611, 1986.
6. Kim C. H. and Childs D. W., "Analysis for Rotordynamic Coefficients of Helically-Grooved Turbulent Annular Seals", ASME Journal of Tribology, Vol. 109, pp. 136-143, 1987.
7. Childs D. W., "The Space Shuttle Main Engine High-Pressure Fuel Turbopump Rotordynamic Instability Problem", ASME Journal of Engineering for Power, Vol. 100, pp. 49-57, 1978.
8. Kalmykov G. P., "Critical Speed of Shaft Stress Analysis of Pumps and Turbine (2D/3D)", Technical Report, CONTRACT No. HYSA-99-S001, 2000.
9. Black H. F. and Jenssen D. N., "Dynamic Hybrid Properties of Annular Pressure Seals", Proceeding of Journal Mechanical Engineering, Vol. 184, pp. 92-100, 1970.
10. Black H. F. and Jenssen D. N., "Effects of High-Pressure Ring Seals on Pump Rotor Vibrations", ASME paper No. 71-WA/FF-38, 1971.
11. Black H. F., Allaire P. E. and Barrett L. E., "Inlet Flow Swirl in Short Turbulent Annular Seal Dynamics", 9th International Conference on Fluid Sealing, pp. 1-3, 1981.
12. Kim C. H., "Analysis and Testing for Rotordynamic Coefficients of Grooved Turbulent Annular Seals", Ph. D. Thesis, Dept. of Mechanical Engineering, Texas A&M University, 1985.
13. Ha T. W., Lee Y. B. and Kim C. H., "Leakage and rotordynamic analysis of a high pressure floating ring seal in the turbo pump unit of a liquid rocket engine", Tribology International, accepted to be published, 2001.
14. Nelson C. and Nguyen D., "Analysis of eccentric annular incompressible seals: Part 1-a new solution using Fast Fourier Transforms for determining hydrodynamic forces", Transactions of the ASME, Vol. 52, pp. 1-6, 1987.
15. Ha T. W. and Lee A. S., "A Modeling of Pump Impeller Shroud and Wear-Ring Seal as a Whole, and Its Application to the Pump Rotordynamics", KSME International Journal, Vol. 12(3), pp. 441-450, 1998.
16. Thomas H., "Instabile Eigenschwingungen von Turbinelaufern angefacht durch die Spaltstromungen Stopfbuschen und Beschauflungen", Bull de L?AIM, Vol. 71, pp. 317-328, 1958.
17. Alford J., "Protecting Turbomachinery from Self-Excited Rotor Whir", ASME Journal of Engineering for Power, pp. 333-344, 1965.
18. Bolleter U., Leibundhut E., Sturchler R. and McCloskey T., "Hydraulic Interaction and Exciatation Forces of High Head Pump Impellers", Proceedings of the Third Joint ASCE/ASME Mechanics Conference, La Jolla, CA, pp. 197-194, 1989.

Nomenclature

A	$((b_1 + \sqrt{d_e\delta})n)/D_{CP}$
b	width of ball bearing
b_e	width of groove in elastic-ring
b_1	width of elastic-ring
C	direct damping
c	cross-coupled damping
D	outer diameter of ball bearing
D_1	inner diameter of elastic-ring
D_2	outer diameter of elastic-ring
D_{CP}	$(D_1 + D_2)/2$
D_m	mean blade diameter of turbine
d	inner diameter of ball bearing
d_e	diameter of curvature of groove in elastic-ring
E	Young's modulus
K	direct stiffness
k	cross-coupled stiffness

L_t turbine blade height
n number of groove in elastic-ring
s $b/2 - 2/\delta$
s_b $s + \delta$
T turbine torque
α compliance of elastic-ring
β change in thermodynamic efficiency per unit of rotor displacement
δ depth of groove in elastic-ring
ω rotational frequency